Ring-Opening Polymerization of Lactides Initiated by Zinc Alkoxides Derived from NNO-Tridentate Ligands

Hsuan-Ying Chen, Hui-Yi Tang, and Chu-Chieh Lin*

Department of Chemistry, National Chung-Hsing University, Taichung 402, Taiwan, R.O.C.

Received March 2, 2006; Revised Manuscript Received March 30, 2006

ABSTRACT: A new series of dinuclear zinc complexes of the types $[LZnEt]_2$ and $[LZn(\mu\text{-}OBn)]_2$ (where L = NNO-tridentate Schiff base ligand) have been prepared. The activities of zinc alkoxides, $[LZn(\mu\text{-}OBn)]_2$, toward the ring-opening polymerization of L-lactide have been investigated. Experimental results indicate that the reactivity of $[LZn(\mu\text{-}OBn)]_2$ was dramatically affected by both the electronic and steric effect of the substituents on the Schiff base. The polymerization kinetics using $[L^1Zn(\mu\text{-}OBn)]_2$ (**2a**) as an initiator were also studied, and the experimental results reveal that the rate of reaction is first-order, which depends on both [LA] and $[L^1Zn(\mu\text{-}OBn)]_2$. Furthermore, the heterotactic PLA with *Pr* up to 91% can be achieved by initiating of $[L^5Zn(\mu\text{-}OBn)]_2$ in CH_2Cl_2 at −55 °C.

Introduction

Poly(lactide) (PLA) and its copolymers have been studied intensively because of their vast potential applications in many fields.[1] Ring-opening polymerization (ROP) of lactides to form polylactides by single-site metal alkoxide precursors has attracted considerable recent attention since the properties of a given PLA are determined by its molecular weight, molecular weight distribution, and molecular microstructure. However, various modes of strategies have been used for the preparation of PLA, a precursor for the synthesis of ring-opening polymerization of lactide. Earlier, many metal complexes (e.g., Al[2], Li[3], Mg[4], Fe[5], Sn[6], and Zn[7]) have been used as initiators/catalysts for ROP of cyclic esters. However, in many cases, backbiting reaction/transesterification takes place as side reactions, resulting in the formation of macrocycles with a wide range of molecular weight distribution. The undesired backbiting/transesterification reactions can be minimized by using a bulky ligand coordinatively attached with active metal center which provides of a steric barrier for prevention of undesired side reactions. Recently, many coordinately bulky metal complexes have been synthesized in order to increase a mononuclear active site.[2,6,7] The factor responsible for mechanistic approaches to control the side reaction from transesterification and chain transfer is not well understood during initiating ring-opening polymerization with stereoselectivity.[2n−p,4e]

Because of their diverse forms and ease of preparation, many Schiff base supported metal complexes have been widely used as catalysts in many applications.[8] However, their application in ROP is not been explored thoroughly. The first Schiff base zinc complex was used as an initiator for polymerization of L-lactide by Chisholm et al.[7c] Recently, Gibson's group[6d] developed an unusual tetradentate ligand by attacking amide at the imine carbon atom of tridentate Schiff base ligands. A reverse process disassembles the so-formed tetradentate ligands, affording single-site initiators for lactide polymerization. Most recently, Justyniak[2m] described a simple method for the synthesis of alkylaluminum and alkoxyaluminum cationic species by employing inexpensive reagents.

It has been well-known that the Schiff base zinc complexes of the type [LZnX] in which X = dextrous alkyloxide were forecasted to be the most active site for ROP of lactide due to their basic nature compared to bulky aryloxide. Absence of steric bulk in X will lead to L_2Zn by disproportionation. Hereby, we describe the preparation of a series of NNO-tridentate Schiff base ligands (Chart 1) to avoid disproportionation and to increase aryloxide basicity by the decreasing Lewis acid character of central metal with the help of increasing the coordination number of Zn. The catalytic activities of zinc alkoxides with different substituents on the phenol group of N,N,O−tridentate Schiff base ligands will also be discussed in detail.

Chart 1

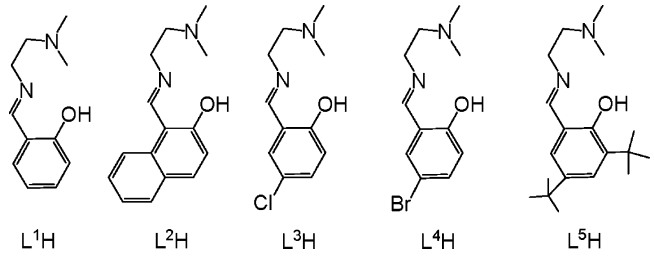

Results and Discussion

Synthesis and Solid-State Structural Determination. Reaction of (*E*)-2-[(2-(dimethylamino)ethylimino)methyl]phenol (L^1-H) with $ZnEt_2$ produced a dimeric zinc complex $[L^1ZnEt]_2$ (**1a**) in moderate yield. Further reaction of **1a** with benzyl alcohol (BnOH) leads to the formation of $[L^1Zn(\mu\text{-}OBn)]_2$ (**2a**). Unlike other Schiff base ligands,[7c] L^1-H is able to provide strong coordination from the amino group to Zn atom and therefore stabilizes the zinc alkoxide, $[L^1Zn(\mu\text{-}OBn)]_2$, without further disproportionation. The stability of $[L^1Zn(\mu\text{-}OBn)]_2$ provides us an opportunity to investigate both the electronic and steric effect for the ring-opening polymerization of lactides. Several NNO-tridentate-type Schiff base ligands (L^2−L^5H) with different substituents on phenyl group were prepared. $[L^2ZnEt]_2$ (**1b**), $[L^3ZnEt]_2$ (**1c**), $[L^4ZnEt]_2$ (**1d**), and $[L^5ZnEt]_2$ (**1e**) were synthesized by a method similar to that of **1a**, as shown in Scheme 1. In addition, $[LZnOBn]_2$ (L = L^2−L^5) (**2b**−**2e**) could also be synthesized by the foregoing way.

X-ray single-crystal structure analysis of $[L^2ZnEt]_2$ (**1b**) (Figure 1) showed a dimeric behavior with pentacoordination around the zinc center bridged through the oxygen atom of the Schiff base ligands, and the geometry around Zn atom was a

10.1021/ma060471r CCC: $33.50
Published on Web 05/02/2006

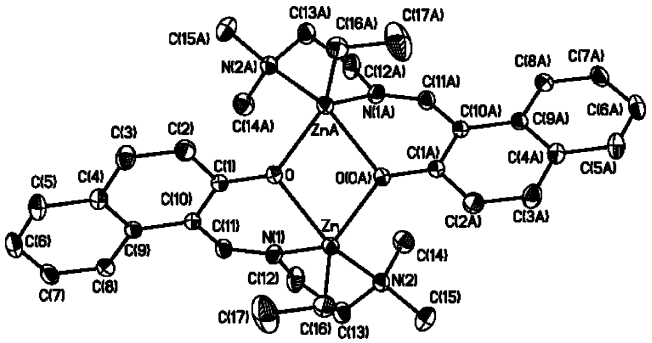

Figure 1. ORTEP drawing of $[L^2ZnEt]_2$ (**1b**) (non-hydrogen atoms) with thermal ellipsoids drawn at the 20% probability level.

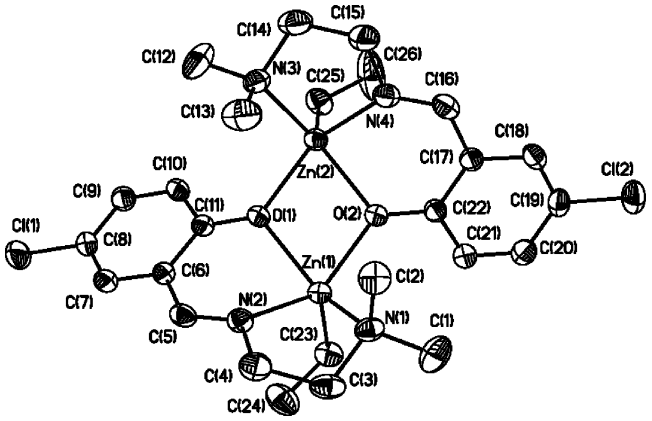

Figure 2. ORTEP drawing of $[L^3ZnEt]_2$ (**1c**) (non-hydrogen atoms) with thermal ellipsoids drawn at the 20% probability level.

distorted tetragonal pyramid with the ethyl group lying on the axial position and two nitrogen atoms and two oxygen atoms on the basal position. The Zn atom is ca. 0.86 Å above the N(1)N(2)OO(0A) mean plane with an average compressed axial O−Zn−N(2) bond angle of 139.75(9)° and equatorial N(1)−Zn−O(0A), N(1)−Zn−C(16), and O(0A)−Zn−C(16) bond angles of 123.61(9)°, 115.27(12)°, and 120.32(12)°. The distances between the Zn atom and O, O(0A), C(16), N(1), and N(2) were 2.178(2), 2.061(2), 2.008(3), 2.113(3), and 2.289(2) Å. The structure of $[L^3ZnEt]_2$ (**1c**) (Figure 2) is an analogue of **1b** with the average compressed axial O(1)−Zn(2)−N(4) and O(2)−Zn(1)−N(2) bond angle of 132.64(9)° and 132.47(12)° and equatorial N(3)−Zn(2)−O(2), N(3)−Zn(2)−C(25), O(2)−Zn(2)−C(25), N(1)−Zn(1)−O(1), N(1)−Zn(1)−C(23), and O(1)−Zn(1)−C(23) bond angles of 128.40(13)°, 111.95(12)°, 118.49(12)°, 129.01(12)°, 109.12(17)°, and 120.71(17)°. The distances from the Zn(1) atom to O(1), O(2), C(23), N(1), and N(2) were 2.137(3), 2.066(3), 1.985(4), 2.284(3), and 2.168(3)

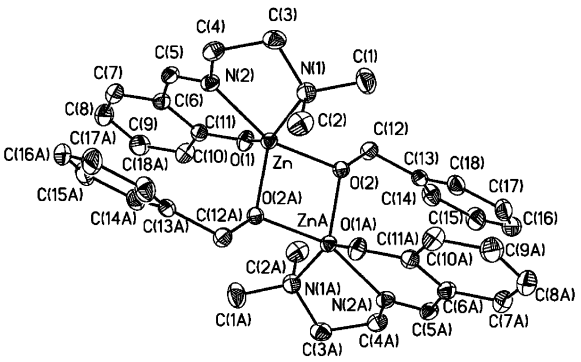

Figure 3. ORTEP drawing of $[L^1Zn(\mu\text{-OBn})]_2$ (**2a**) (non-hydrogen atoms) with thermal ellipsoids drawn at the 20% probability level. Selected bond lengths (Å) and bond angles (deg): Zn−O(1) 2.0273-(2), Zn−O(2) 2.016(1), Zn−O(2A) 1.978(2), Zn−N(1) 2.324(2)and Zn−N(2) 2.067(2). O(2)−Zn−N(2) 157.06(7), N(1)−Zn−O(1) 149.06-(8), N(1)−Zn−O(2A) 106.31(8) and O(2A)−Zn−O(1) 92.19(7).

Å. The distances from the Zn(2) atom to O(1), O(2), C(25), N(3), and N(4) were 2.084(3), 2.128(3), 1.989(4), 2.261(3), and 2.199(4) Å. X-ray analysis of $[L^4ZnEt]_2$ (**1d**) showed a dimer similar to that of **1b**.

The molecular structure of **2a** (Figure 3) reveals a dimeric behavior with two symmetrical pentacoordinated zinc center bridging through the oxygen atom of the benzyl alkoxy group, and the geometry around Zn atoms were distorted trigonal bipyramidal with an average compressed axial O(2)−Zn−N(2) bond angle of 157.06(7)° and equatorial N(1)−Zn−O(1), N(1)−Zn−O(2A), and O(2A)−Zn−O(1) bond angles of 149.06(8)°, 106.31(8)°, and 92.19(7)°. The distances from the Zn atom to O(1), O(2), O(2A), N(1), and N(2) were 2.0273(2), 2.016(1), 1.978(2), 2.324(2), and 2.067(2) Å, respectively. The structure of $[L^2Zn(\mu\text{-OBn})]_2$ (**2b**) is analogous to that of **2a**. $[(L^4)_2Zn]$ (**3**) was obtained from the recrystallization of a $[L^4Zn(\mu\text{-OBn})]_2$ (**2d**) solution due to disproportionation. X-ray analysis of **3** (Figure 4) showed it is a four-coordinate zinc complex in which the Zn atom was distorted tetrahedral with the N(2)−Zn(1)−N(4) and O(1)−Zn−O(2) bond angles of 156.6(4)° and 95.1(4)°. The distances between Zn(1) and N(2), N(4), O(1), and O(2) were 2.041(9), 2.037(9), 2.007(9), and 1.998(9) Å, respectively.

To explore the possible mechanism of ROP reaction of lactide initiated by $[LZn(\mu\text{-OBn})]_2$, the reaction of 2-(dimethylamino)-ethanol with $[L^5ZnEt]_2$ (**1e**) was performed as shown in Scheme 2. $[L^5Zn(\mu\text{-}OCH_2CH_2NMe_2)]_2$ (**4**) was synthesized and offers momentous information about the polymerization reactions and its mechanism. The molecular structure of **4** (Figure 5) demonstrated a dimeric character in which the Zn atoms has a distorted trigonal-bipyramidal structure with an average compressed axial O(1)−Zn(1)−O(2A) bond angle of 168.93(14)°

Scheme 1. Preparation of Compounds 1 and 2

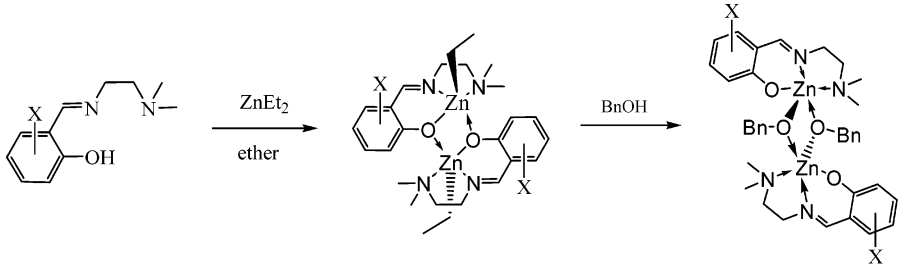

1a: X = 4-H
1b: X = 3,4-naphthalyl
1c: X = 4-Cl
1d: X = 4-Br
1e: X = 4,6-di-^{t}Bu

2a: X = 4-H
2b: X = 3,4-naphthalyl
2c: X = 4-Cl
2d: X = 4-Br
2e: X = 4,6-di-^{t}Bu

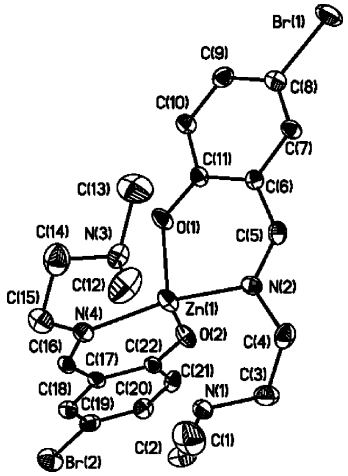

Figure 4. ORTEP drawing of $(L^4)_2Zn$ (**3**) (non-hydrogen atoms) with thermal ellipsoids drawn at the 20% probability level.

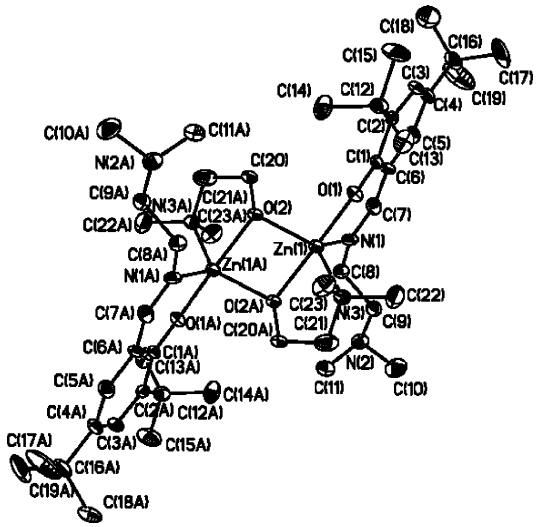

Figure 5. ORTEP drawing of $[L^5Zn(\mu\text{-}OCH_2CH_2NMe_2)]_2$ (**4**) (non-hydrogen atoms) with thermal ellipsoids drawn at the 20% probability level.

Scheme 2. Preparation of Compound 4

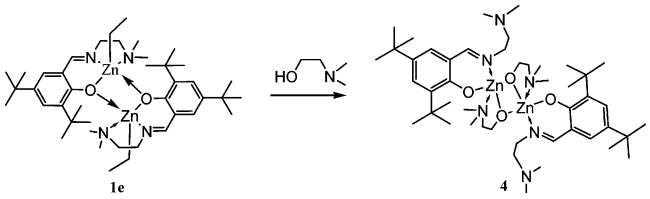

and equatorial N(3)−Zn(1)−O(2), N(1)−Zn(1)−O(2), and N(3)−Zn(1)−N(1) bond angles of 125.59(16)°, 115.25(16)°, and 118.20(17)°. The distances from the Zn(1) atom to O(1), O(2), O(2A), N(1), and N(3) were 2.013(3), 1.989(3), 2.089(3), 2.037(4), and 2.146(4) Å, respectively.

^{1}H NMR Studies at Variable Temperature. The solid-state structure of $[L^1Zn(\mu\text{-}OBn)]_2$ (**2a**) shows a dimeric behavior. However, there are three most possible isomers (only listed the most possible and stable isomers) for **2a**, as shown in Chart 2. The ^{1}H NMR spectrum of **2a** (Figure 6) in d_8-toluene at 20 °C shows two sets of resonance peaks with a ratio of ca. 10/1, indicating the existence of both dimeric and monomeric species instead feature in solution at this temperature. However, three sets of resonance peaks were observed for **2b**. Variable temperature NMR studies of **2a** were performed, and experimental results revealed that a new set of resonance peaks occur

Chart 2

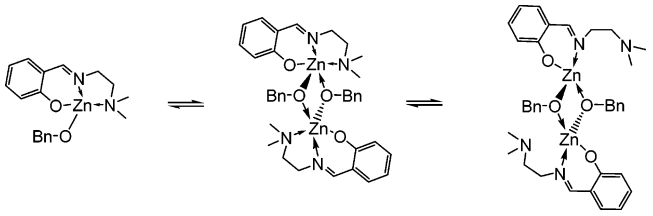

when the temperature was heated at 80 °C. These three isomers are at fast equilibrium above 100 °C on the NMR scale (Figure 7). It is interesting to note that while the solution was cooled from 100 to 20 °C for 2 days, the ratio of these two isomers remains the same as the sample prior heating. Both compounds act as precursors for the ring-opening polymerization of lactides.We attribute the rate of initiation of ROP by a combination of the basicity of RO^- ligands, electrophilicity of the metal centers, and the nature of the geometry of the transition state at the metal center.

Melting Point Depression Study of 2a. Based on the variable NMR studies of **2a**, two isomers exist in solution at 80 °C. To figure out which two isomers are possible, freezing point depression studies of **2a** using naphthalene as the solvent were performed. Experimental results reveal the activity $i = 1.18 \pm 0.16$, indicating the existence of ca. 82% of dimer and 18% of monomer. This result is consistent with ^{1}H NMR experiment results in which the ratio between two isomers is 6/1.

Polymerization of L-Lactide. Polymerization of L-lactide using **2a** (2.5 mM) as an initiator was systematically investigated in toluene (Table 1). From Table 1, we found that the complex **2a** is an efficient initiator for the polymerization of L-lactide. The polymerization goes to completion within 30 min at 20 °C. On the basis of the molecular weight of poly(L-lactide) (PLLA) and $[LA]_0/[\mathbf{2a}]$ ratio, we believed that all of the these two BnO^- groups could be used as initiators. The linear increase in M_n with conversion and the low polydispersity index (PDI, M_w/M_n) of the polymers revealed that the level of polymerization control was high.[9] The ^{1}H NMR spectrum of PLLA prepared using a $[LA]_0/[\mathbf{2a}]$ ratio of 50 showed one benzyl ester and one hydroxy chain end with an integral ratio of 5:1 between He and Hc, suggesting that the initiation occurred through the insertion of the benzyl alkoxy group from **2a** into L-lactide.[10] We can conclude that the observed rate order for the initial rate of ring-opening of L-lactide represents a combination of electronic and steric factors.

To realize the electronic and steric effect of the substituent on the Schiff base affecting the activity of zinc complexes, the activities of **2b**−**2e** complexes toward ROP of L-lactide were also examined, as shown in Table 2. Experimental results show that all complexes efficiently initiate the polymerization of L-lactide, and PLLA was obtained with the expected molecular weight and with low polydispersity, hereby supporting that the reactivity varies with different functional groups on the ligand. No difference in chemical activities was observed by changing from the phenyl to naphthalenyl group due to little difference in their electronic effects (entries 1 and 2). When the para-hydrogen atom was replaced by an electron-withdrawing group such as Br or Cl atom, the reactivity also decreases due to increase in electronegativity of the substituent (entries 1, 3, and 5). For instance, the conversion up to 91% can be achieved within 30 min using **2a** as an initiator. Whereas by using **2c** (**2d**) as an initiator, the reaction takes 240 (50) min. This phenomenon could be attributed to the more electronegative behavior of the substituent on the ligand; the stronger the zinc

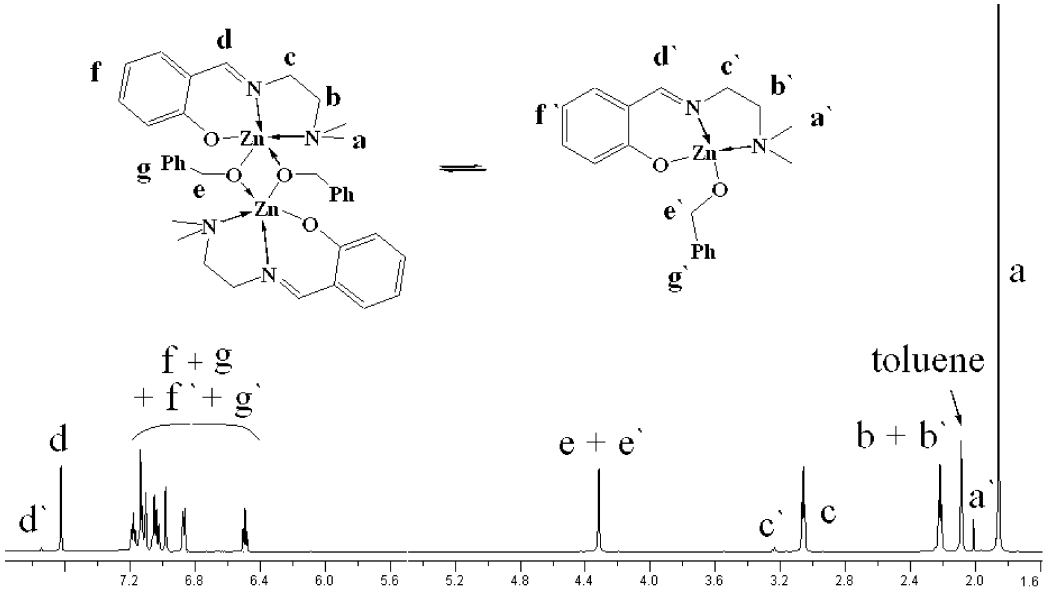

Figure 6. ^{1}H NMR spectrum of [L^{1}Zn(μ-OBn)]$_2$ (**2a**) in d_8-toluene at 20 °C.

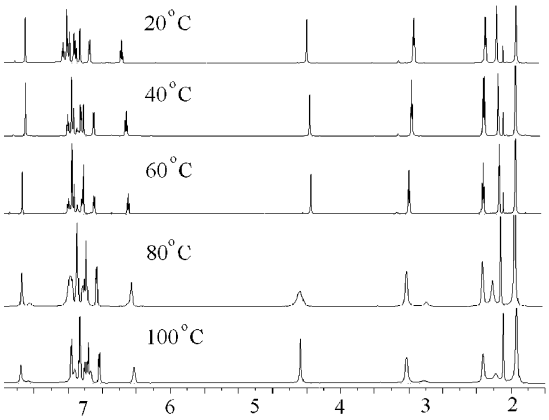

Figure 7. ^{1}H NMR spectrum of [L^{1}Zn(μ-OBn)]$_2$ (**2a**) in d_8-toluene with variable temperature.

alkoxide bond, therefore the slower the reaction rate. Indirect evidence came from the comparison of the Zn−C (ethyl) bond distance of the molecular structures **1b**, **1c**, and **1d.** A better evidence would be by comparing the molecular structures of **2a**−**2d**; however, the **2c** and **2d** compounds fail to crystallize. The Zn−C (ethyl group) bond distance decreases from 2.008(3) Å for **1b** to 2.026(9) Å for **1d** (Br) and 1.985(4) Å for **1c** (Cl).

When an ortho-hydrogen is replaced by a much more sterically hindered *tert*-butyl group, the polymerization rate also decreases dramatically as compared to the reaction rate of **2a** and **2e**. We proposed a sterically hindered ligand resists the approaching of a monomer toward zinc center, therefore retarding the reaction rate. This is in contrast to the results observed in an aluminum diol system in which a sterically more hindered ligand increases the polymerization rate.[2c] Further investigation is in progress.

Kinetic and Mechanistic Studies of Polymerization of l-Lactide by 2a. A kinetic study was conducted in order to establish reaction order for the polymerization of L-lactide with **2a**. Conversion of L-lactide ([LA] = 0.69 M in 2 mL of $CDCl_3$) with time was monitored by ^{1}H NMR for various concentrations of **2a** ([**2a**] = 4.33, 6.89, 10.60, and 12.36 mM) at 25 °C until monomer consumption was completed. Plots of ($\ln[LA]_0 - \ln[LA]$) vs time in a wide range of $[LA]_0$ were linear, indicating polymerization proceeds with first-order dependence on monomer concentration (Figure 8). To determine the kinetic order in **2a**, the dependence of k_{obs} on $[LA]_0$ was analyzed. Thus, the rate of polymerization could be written as $-d[LA]/dt = k_{obs}[LA]$, where $k_{obs} = k[\mathbf{2a}]^x$ and k was the rate constant. Plotting ln k_{obs} vs ln [**2a**] allowed us to determine x, the order in [**2a**] concentration. From the slope of the fitted line as shown in Figure 9, the rate constant $k = 40.896\ M^{-1}\ min^{-1}$. Therefore, on the basis of this analysis, $\chi = 1$. The reaction is first-order in [**2a**] and monomer concentrations, and the overall rate equation is $-d[LA]/dt = k[LA]^1[\mathbf{2a}]^1$.

Though [LZn(μ-OBn)]$_2$ is a dimeric pentacoordinated compound in the solid state, it exists as an equilibrium between a dimer and a monomer in solution according to the ^{1}H NMR studies. The molecular structure of **4** indicates that the bond strength between Zn−N of amine group is weaker than that of Zn−OBn bond of μ-alkoxide. The kinetic studies show the reaction rate is first-order proportional to both [LA] and [**2a**]. Therefore, the reaction mechanism was proposed as shown in Scheme 3. L-Lactide coordinates to the monomeric four-coordinated zinc alkoxide **A**, yielding a pentacoordinated intermediate **B**, followed by the insertion of a benzylalkoxy group into L-lactide to produce a new initiator **C**.

Stereoselectivity of *rac*-LA. It has been known that the physical and degradation properties of PLA are dramatically dependent on the stereochemistry of PLA.[11] For example, poly(L-lactide) is a semicrystalline polymer with a melting point around 180 °C. However, poly(*meso*-lactide) is an amorphous polymer. In addition, the equivalent mixture of PLLA and PDLA forms a crystalline stereocomplex with a melting temperature at 230 °C. Kasperczyk et al. have reported that ROP of *rac*-lactide using LiO^tBu gives enriched PLA in a heterotactic sequence.[12] Therefore, the polymerizations of *rac*-LA initiated by zinc alkoxide complexes **2a**, **2b**, **2d**, and **2e** are also performed, and the stereoselectivity is determined by the homonuclear decoupled ^{1}H NMR spectra. By changing the solvent from CH_2Cl_2 to THF at 25 °C resulted in a little decrease in *Pr* (probably due to the racemic linkages between monomer units)[13] and reaction rates (Table 3). It was worthwhile to note that the tacticity of the polymer was significantly influenced by the ligand used and temperature. For instance, changing the ligand from L^1 to a sterically bulkier ligand L^5 at 25 °C resulted in an increase in *Pr* from 59% to 74% (entries 1 and 5, Table

Table 1. Polymerization of L-Lactide in Toluene (20 mL) Using Complex 2a (2.5 mM) as an Initiator

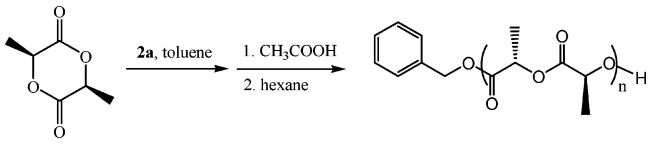

entry	$[M]_0/[\mathbf{2a}]$	T (°C)	t (min)	conv[a] (%)	M_n(calc)[b]	M_n(GPC)[c]	M_n(NMR)[a]	PDI[c]
1	50	20	30	90	3300	4300	3200	1.12
2	100	20	30	92	6700	11100	6500	1.05
3	120	20	30	89	7800	12300	8300	1.04
4	150	20	30	91	9900	17400	9500	1.04
5	200	35	25	99	14400	29700	—[d]	1.03
6[e]	600	20	140	98	42000	78000	—[d]	1.11
7	50 (50)	20	(60, 120)	89	6500	9700	7000	1.05

[a] Obtained from ^{1}H NMR analysis. [b] Calculated from the molecular weight of LA × $[M]_0/2[\mathbf{2a}]_0$ × conversion yield + M_w(BnOH). [c] Obtained from GPC analysis and calibrated by polystyrene standard. [d] Signals for benzyl alkoxy group are too small to be calibrated. [e] $[\mathbf{2a}] = 2.65$ mM, in 20 mL of CH_2Cl_2.

Table 2. Polymerization of L-Lactide (375 mM) in Toluene (20 mL) Using Complexes 2a−2e (2.5 mM) as Initiators at 25 °C

entry	initiator	t (min)	conv[a] (%)	M_n(calc)[b]	M_n(NMR)[a]	M_n(GPC)[c]	PDI[c]
1	**2a**	30	91	9 900	9 500	17 400	1.04
2	**2b**	30	94	10 300	10 600	18 600	1.04
3	**2c**[d]	240	90	9 800	10 900	22 100	1.09
4	**2d**	30	60				
5	**2d**	50	92	10 000	9 400	17 900	1.04
6	**2e**	30	41				
7	**2e**	80	93	10 200	12 000	21 500	1.08

[a] Obtained from ^{1}H NMR analysis. [b] Calculated from the molecular weight of LA × $[M]_0/2[\text{initiator}]_0$ × conversion yield + M_w(BnOH). [c] Obtained from GPC analysis and calibrated by polystyrene standard. [d] Performed at 80 °C.

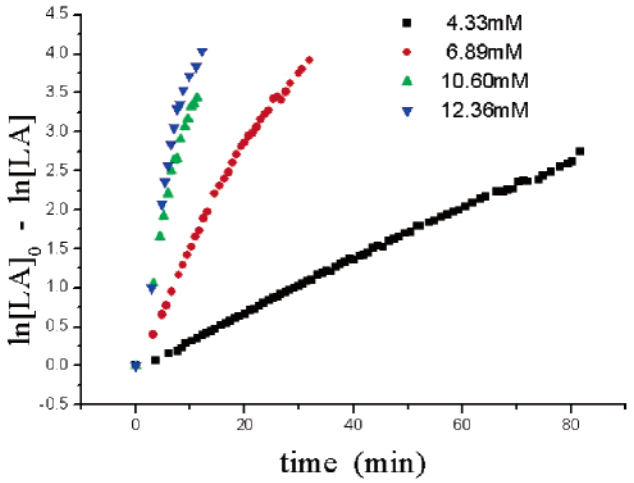

Figure 8. First-order kinetic plots for L-lactide polymerizations with time in $CDCl_3$ with different concentration of $[L^1Zn(\mu\text{-OBn})]_2$ as an initiator.

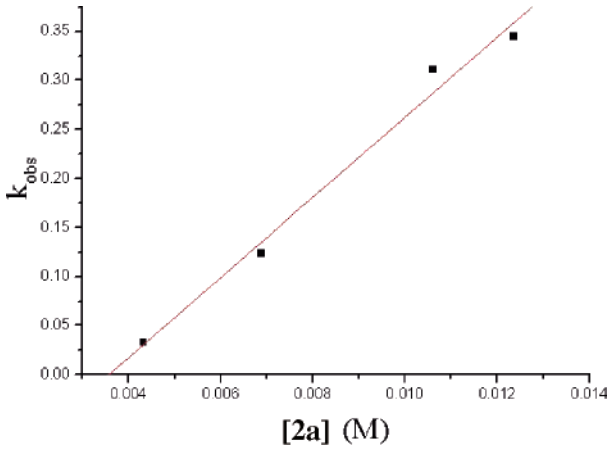

Figure 9. Linear plot of k_{obs} vs $[L^1Zn(\mu\text{-OBn})]_2$ for the polymerization of L-lactide with $[LA]_0 = 0.69$ M in $CDCl_3$. $k = 40.896$ M^{-1} s^{-1}.

3). Lowering the temperature from 25 to 0 °C increased *Pr* from 74% to 86%. Furthermore, the heterotactic PLA with *Pr* up to 91% can be achieved at −55 °C (entry 6, Table 3 and Figure 10). We conclude that increasing the steric group in the ortho positions of phenol group could promote the stereoselectivity for ROP of *rac*-LA by these types of initiators. Further investigation by using a sterically bulky ligands in progress.

Conclusions

A series of NNO-tridentate Schiff base ligands (L^1-H−L^5-H) and their zinc alkyl and zinc alkoxide complexes have been synthesized. All zinc alkoxide complexes have shown great reactivities toward the controlled polymerization of LA, and the reactivity increases with the help of the electron-donating group on the phenyl ring. However, a sterically bulky ligand hindered the reaction rate. We have also found that the polymerization reaction proceeds with first-order rate dependence on both the monomer and initiator concentrations. Complex **2e** has shown good stereoselectivity for ROP of *rac*-lactide in CH_2Cl_2 at low temperature. Much work needs to be done to gain a full understanding of the factors that are truly important in the molecular design of single-site catalyst precursors for stereoselective ROP of lactides.

Experimental Section

General. All manipulations were carried out under a dry nitrogen atmosphere. Solvents, benzyl alcohol, L-lactide, and deuterated solvents were purified before use. ^{1}H and ^{13}C NMR spectra were recorded on a Varian Unity Inova-600 (600 MHz for ^{1}H and 150 MHz for ^{13}C) or a Varian Mercury-400 (400 MHz for ^{1}H and 100 MHz for ^{13}C) spectrometer with chemical shifts given in ppm from the internal TMS or center line of $CHCl_3$. Microanalyses were performed using a Heraeus CHN-O-RAPID instrument. The GPC measurements were performed on a Hitachi L-7100 system equipped with a differential Bischoff 8120 RI detector using THF (HPLC grade) as an eluent. Molecular weight and polydispersity of PLA were calculated using polystyrene as a standard reference.

Scheme 3. Proposed Mechanism for the ROP of L-Lactide Initiated by 2a

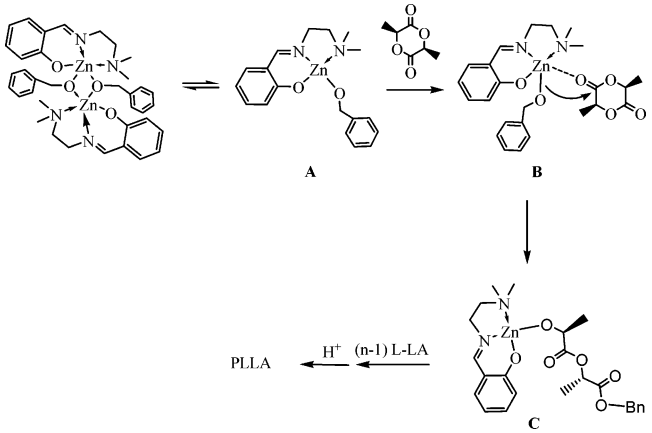

(*E*)-2-((2-(Dimethylamino)ethylimino)methyl)phenol (L^1-H)[2n,14] and (*E*)-2,4-di-*tert*-butyl-6-((2-(dimethylamino)ethylimino)methyl)-phenol (L^5-H)[15] were prepared by acid-catalyzed condensation following literature procedures.

Synthesis of (*E*)-1-((2-(Dimethylaminoethylimino)methyl)-naphthalen-2-ol (L^2-H). A mixture of N^1,N^1-dimethylethane-1,2-diamine (8.8 g, 100 mmol), 2-hydroxynaphthalene-1-carbaldehyde (17.2 g, 100 mmol), and HCl (0.30 mL) were stirred in absolute THF (30 mL) for 1 day. Volatile materials were removed under vacuum to give dark yellow powder. Yield: 21.3 g (88%). ^{1}H NMR ($CDCl_3$, 400 MHz): δ 8.75 (1H, s, N=C**H**), 7.83 (1H, d, J = 8.0 Hz, Ar**H**), 7.67 (1H, d, J = 9.6 Hz, Ar**H**), 7.60 (1H, d, J = 7.6 Hz, Ar**H**), 6.91 (1H, d, J = 9.2 Hz, Ar**H**), 7.43 (2H, t, J = 8.4 Hz, Ar**H**), 7.23 (2H, t, J = 7.6 Hz, Ar**H**), 3.67 (2H, t, J = 6.4 Hz, C=NC**H$_2$**), 2.65 (2H, t, J = 6 Hz, C=NCH$_2$**H$_2$**NMe$_2$), 2.34 ppm (6H, s, N(C**H$_3$**)$_2$). ^{13}C NMR ($CDCl_3$, 400 MHz): δ 162.00 (**C**=N), 158.08 (**C**OH) 137.26, 133.87, 129.20, 127.87, 126.14, 125.17, 122.57, 117.73, 106.55 (Ar), 59.36 (CC=N**C**H$_2$), 50.73 (CC=NCH$_2$**C**H$_2$), 45.60 ppm (N(**C**H$_3$)$_2$).

Synthesis of (*E*)-4-Chloro-2-((2-(dimethylamino)ethylimino)-methyl)phenol (L^3-H). N^1,N^1-Dimethylethane-1,2-diamine (8.8 g, 100 mmol), 5-chloro-2-hydroxybenzaldehyde (15.6 g, 100 mmol), and HCl (0.30 mL) were stirred in absolute ether (30 mL) for 1 day. Volatile materials were removed under vacuum to give light yellow powder. Yield: 20.8 g (92%). ^{1}H NMR ($CDCl_3$, 400 MHz): δ 8.29 (1H, s, N=C**H**), 7.23 (1H, dd, J = 8.4, 2.4 Hz, Ar**H**), 7.22 (1H, d, J = 2.4 Hz, Ar**H**), 6.89 (1H, d, J = 8.4 Hz, Ar**H**), 3.72 (2H, t, J = 6.4 Hz, C=NC**H$_2$**), 2.64 (2H, t, J = 6.0 Hz, C=NCH$_2$**H$_2$**NMe$_2$), 2.29 ppm (6H, s, N(C**H$_3$**)$_2$). ^{13}C NMR ($CDCl_3$, 400 MHz): δ 164.33 (**C**=N), 159.83 (**C**OH), 131.96, 130.29, 122.92, 119.44, 118.56 (Ar), 59.66 (CC=N**C**H$_2$), 57.56 (CC=NCH$_2$**C**H$_2$), 45.73 ppm (N(**C**H$_3$)$_2$). (EI, *m*/*e*): 226 (M, 1.31%). Anal. Calcd (found) for $C_{11}H_{15}ClN_2O$: C 58.28 (58.12), H 6.67 (6.72), N 12.36 (12.07)%.

Synthesis of (*E*)-4-Bromo-2-((2-(dimethylamino)ethylimino)-methyl)phenol (L^4-H). Using a method similar to that for L^3-H but 5-bromo-2-hydroxybenzaldehyde (15.6 g, 100 mmol) was used as reagent and diethyl ether as solvent. Yield: 24.30 g (90%). ^{1}H NMR ($CDCl_3$, 400 MHz): δ 8.28 (1H, s, N=C**H**), 7.36 (1H, dd, J = 8.8, 2.4 Hz, Ar**H**), 7.34 (1H, d, J = 2.4 Hz, Ar**H**), 6.84 (1H, d, J = 8.8 Hz, Ar**H**), 3.71 (2H, t, J = 6.8 Hz, C=NC**H$_2$**), 2.62 (2H, t, J = 6.8 Hz, C=NCH$_2$C**H$_2$**NMe$_2$), 2.29 (6H, s, N(C**H$_3$**)$_2$) ppm. ^{13}C NMR ($CDCl_3$, 400 MHz): δ 164.23 (**C**=N), 160.34 (**C**OH), 134.75, 133.27, 120.05, 119.01, 109.77 (Ar), 59.63 (CC=N**C**H$_2$), 57.50 (CC=NCH$_2$**C**H$_2$), 45.70 ppm (N(**C**H$_3$)$_2$). (EI, *m*/*e*): 270 (M, 1.04%) Anal. Calcd (found) for $C_{11}H_{15}BrN_2O$: C 48.72 (48.74), H 5.58 (5.35), N 10.33 (10.32)%.

Synthesis of [L^1ZnEt]$_2$ (1a). To a suspension of L^1-H (1.92 g, 10 mmol) in toluene (15 mL) was added diethylzinc (11 mL, 11 mmol). After being stirred at 0 °C for 3 h, a turbid solution was obtained. Volatile materials were removed under vacuum to yield light yellow powder. The powder was washed with hexane (30 mL) twice, and a white powder was obtained after filtration. Yield: 1.85 g (65%). ^{1}H NMR ($CDCl_3$, 400 MHz): δ 8.18 (1H, s, **H**C=N), 7.31, 6.68 (1H, t, J = 7.2 Hz, ArH), 7.15, 6.94 (1H, d, J = 7.6 Hz, ArH), 3.67 (2H, b, C=NC**H$_2$**), 2.66 (2H, b, C**H$_2$**NMe$_2$), 2.32 (6H, s, N(C**H$_3$**)$_2$), 1.10 (3H, t, J = 8.0 Hz, ZnCH$_2$C**H$_3$**), 0.05 (2H, q, J = 8.0 Hz, ZnC**H$_2$**CH$_3$) ppm. ^{13}C NMR ($CDCl_3$, 400 MHz): δ 168.71 (**C**=N), 168.70 (**C**OH), 134.43, 133.82, 122.82, 115.51, 114.70 (Ar), 59.30 (C=N**C**H$_2$), 56.00 (C=NCH$_2$**C**H$_2$NMe$_2$), 45.70 (N(**C**H$_3$)$_2$), 12.91 (ZnCH$_2$**C**H$_3$), −1.48 ppm (Zn**C**H$_2$CH$_3$). Anal. Calcd (found) for $C_{26}H_{40}N_4O_2Zn_2$: C 54.65 (54.28), H 7.06 (7.17), N 9.81 (9.74)%.

Synthesis of [L^2ZnEt]$_2$ (1b). Diethylzinc (11.0 mL, 11.0 mmol) was added to a suspension of (L^2-H) (2.42 g, 10.0 mmol) in CH_2Cl_2 (15.0 mL), and the mixture was stirred at 0 °C for 3 h to produce a dark yellow limpid solution. After 2 h at room temperature, yellow crystals were obtained. The resulting product was collected by filtration and dried in vacuo. Yield: 2.01 g (60%). ^{1}H NMR (d_6-benzene, 400 MHz): δ 8.42 (1H, s, N=C**H**), 7.66 (1H, d, J = 8.4 Hz, Ar**H**), 7.52−7.41 (4H, m, Ar**H**), 7.35 (1H, t, J = 7.2 Hz, Ar**H**), 7.15 (1H, t, J = 7.2 Hz, Ar**H**), 2.90 (2H, t, J = 5.6 Hz, C=NC**H$_2$**), 1.83 (6H, s, N(C**H$_3$**)$_2$), 1.78 (2H, b, C=NCH$_2$**H$_2$**NMe$_2$), 1.68 (3H, t, J = 8.0 Hz, ZnCH$_2$C**H$_3$**), 0.61 ppm (2H, q, J = 8.0 Hz, ZnC**H$_2$**CH$_3$). ^{13}C NMR (*d*-benzene, 400 MHz): δ 170.84 (**C**=N), 162.64 (**C**OH), 135.70, 135.07, 129.35, 127.37, 127.33, 126.64, 121.72, 119.83, 111.14 (Ar), 60.34 (CC=N**C**H$_2$), 55.30 (CC=NCH$_2$**C**H$_2$), 45.55 (N(**C**H$_3$)$_2$), 13.85 (ZnCH$_2$**C**H$_3$), −0.99 ppm (Zn**C**H$_2$CH$_3$). Anal. Calcd (found) for $C_{34}H_{44}N_4O_2Zn_2\cdot 0.8CH_2Cl_2$: C 56.52 (56.64), H 6.22 (6.15), N 7.58 (7.80)%.

Synthesis of [L^3ZnEt]$_2$ (1c). Diethylzinc (11.0 mL, 11.0 mmol) was added to a suspension of (L^3-H) (2.26 g, 10 mmol) in a mixed solution (15 mL) of CH_2Cl_2 (7.5 mL) and THF (7.5 mL). After stirring for 3 h at 0 °C, a green yellow limpid solution was obtained. After 2 h at room temperature, light green crystals were obtained. The resulting product was collected by filtration and dried in vacuo. Yield: 1.60 g (50%). ^{1}H NMR ($CDCl_3$, 400 MHz): δ 8.09 (1H, s, N=C**H**), 7.14 (1H, dd, J = 8.8, 2.4 Hz, Ar**H**), 7.06 (1H, d, J = 2.4 Hz, Ar**H**), 6.83 (1H, d, J = 8.8 Hz, Ar**H**), 3.63 (2H, b, C=NC**H$_2$**), 2.59 (2H, b, C**H$_2$**NMe$_2$), 2.24 (6H, s, N(C**H$_3$**)$_2$), 1.03 (3H, t, J = 8.0 Hz, ZnCH$_2$C**H$_3$**), −0.03 (2H, q, J = 8.0 Hz, ZnC**H$_2$**CH$_3$) ppm. ^{13}C NMR ($CDCl_3$, 400 MHz): δ 166.82 (**C**=N), 166.00 (**C**OH), 133.41, 132.70, 124.15, 121.22, 118.76 (Ar), 59.31 (CC=N**C**H$_2$), 55.61 (CC=NCH$_2$**C**H$_2$), 45.74 (N(**C**H$_3$)$_2$), 12.92 (ZnCH$_2$**C**H$_3$), −1.39 ppm (Zn**C**H$_2$CH$_3$). Anal. Calcd (found) for $C_{26}H_{38}Cl_2N_4O_2Zn_2\cdot 0.2CH_2Cl_2$: C 47.88 (48.09), H 5.89 (5.70), N 8.52 (8.14)%.

Synthesis of [L^4ZnEt]$_2$ (1d). The procedures are similar to that for **1c** with (L^4-H) (2.70 g, 10 mmol) being used. Yield: 2.98 g (82%). ^{1}H NMR ($CDCl_3$, 400 MHz): δ 8.07 (1H, s, N=C**H**), 7.22 (1H, dd, J = 8.0, 2.4 Hz, Ar**H**), 7.17 (1H, d, J = 2.4 Hz, Ar**H**), 6.75 (1H, d, J = 8.0 Hz, Ar**H**), 3.59 (2H, b, C=NC**H$_2$**), 2.55 (2H, b, C**H$_2$**NMe$_2$), 2.19 (6H, s, N(C**H$_3$**)$_2$), 1.00 (3H, t, J = 8.06 Hz, ZnCH$_2$C**H$_3$**), −0.07 ppm (2H, q, J = 8.0 Hz, ZnC**H$_2$**CH$_3$). ^{13}C NMR ($CDCl_3$, 400 MHz): δ 167.35 (**C**=N), 166.77 (**C**OH), 136.01, 135.79, 124.57, 122.15, 105.46 (Ar), 59.24 (CC=N**C**H$_2$), 55.55 (CC=NCH$_2$**C**H$_2$), 45.68 (N(**C**H$_3$)$_2$), 12.99 (ZnCH$_2$**C**H$_3$), −1.34 ppm (Zn**C**H$_2$CH$_3$). Anal. Calcd (found) for $C_{26}H_{38}Br_2N_4O_2Zn_2\cdot 0.2THF$: C 43.73 (43.31), H 5.48 (5.51), N 7.39 (7.28)%.

Synthesis of [L^5ZnEt] (1e). To a suspension of (L^5-H) (3.04 g, 10 mmol) in THF (15 mL) was added diethylzinc (11 mL, 11 mmol). After being stirred for 3 h at 0 °C, a yellow limpid solution was obtained. Volatile materials were removed in vacuo to yield the yellow powder. After adding 30 mL of hexane and washing the powder for 2 h, the yellow powder was collected by filtration. The white solid was obtained and dried in vacuo. Yield: 1.95 g (50%). ^{1}H NMR ($CDCl_3$, 400 MHz): δ 8.16 (1H, s, N=C**H**), 7.38 (1H, s, Ar**H**), 6.87 (1H, s, Ar**H**), 3.69 (2H, b, C=NC**H$_2$**), 2.62 (2H, b, C**H$_2$**NMe$_2$), 2.23 (6H, s, N(C**H$_3$**)$_2$), 1.39 (9H, s, ^{o}C(C**H$_3$**)$_3$), 1.27 (9H, s, ^{p}C(C**H$_3$**)$_3$), 1.20 (3H, t, J = 8.0 Hz, ZnCH$_2$C**H$_3$**), 0.05 ppm (2H, q, J = 8.0 Hz, ZnC**H$_2$**CH$_3$). ^{13}C NMR ($CDCl_3$, 400 MHz): δ 171.24 (**C**=N), 168.60 (**C**OH), 141.22, 134.27, 129.32, 128.80, 117.36 (Ar), 60.07 (CC=N**C**H$_2$), 57.32 (CC=NCH$_2$**C**H$_2$), 46.03 (N(**C**H$_3$)$_2$), 35.46 (^{o}**C**(CH$_3$)$_3$), 33.74 (^{p}**C**(CH$_3$)$_3$), 31.38 (^{o}C(**C**H$_3$)$_3$),

Table 3. Polymerization of *rac*-Lactide (500 mM) in CH_2Cl_2 (10 mL) Using Zinc Alkoxides (2.5 mM) as Initiators

entry	initiator	time	conv[a] (%)	M_n(calc)[b]	M_n(NMR)[a]	M_n(GPC)[c]	PDI[c]	*Pr*[a] (%)
1	**2a**	4 h	97	7100	6700	6300	1.26	59
2	**2a**[d]	12 h	43	4800	3931	3700	1.09	56
3	**2b**	4 h	98	7200	7200	9200	1.14	65
4	**2d**	4 h	95	6900	8200	10700	1.07	65
5	**2e**	6 h	98	7200	9100	10500	1.13	74
6	**2e**[e]	1 week	50	1900	2300	3800	1.06	91

[a] Obtained from ^{1}H NMR analysis. [b] Calculated from the molecular weight of LA × $[M]_0/2[\text{initiator}]_0$ × conversion yield + M_w(BnOH). [c] Obtained from GPC analysis and calibrated by polystyrene standard. [d] Using THF as solvent. [e] [*rac*-LA]/[**2e**] = 100 at −55 °C.

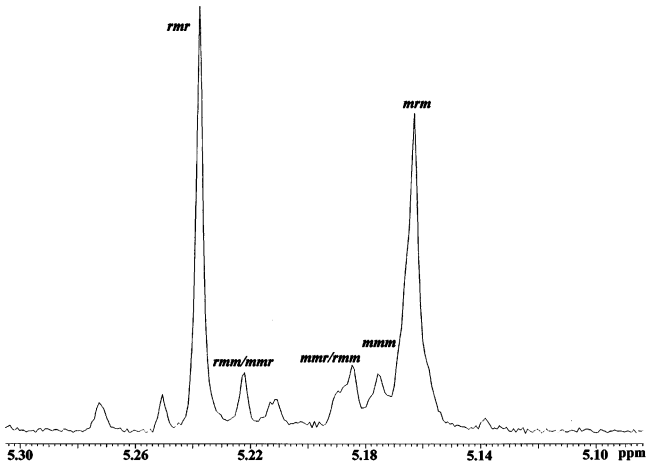

Figure 10. Homonuclear decouple ^{1}H NMR spectrum of the methine region of heterotactic PLA prepared from *rac*-LA with $[L^5Zn(\mu\text{-OBn})]_2$ (**2e**) in CH_2Cl_2 at −55 °C (600 MHz, $CDCl_3$).

29.44 ($^pC(\mathbf{C}H_3)_3$), 12.99 ($ZnCH_2\mathbf{C}H_3$), −1.00 ppm ($Zn\mathbf{C}H_2CH_3$). Anal. Calcd (found) for $C_{42}H_{72}N_4O_2Zn_2$: C 63.39 (63.19), H 7.04 (7.26), N 9.12 (8.89)%.

Synthesis of $[L^1Zn(\mu\text{-OBn})]_2$ (2a). To a suspension of $[L^1ZnEt]_2$ (0.71 g, 1.25 mmol) in THF (15 mL) was added BnOH (0.31 mL, 3.0 mmol) at 0 °C. When the turbid mixture was stirred for 3 h, a yellow limpid solution was obtained, which was then crystallized to yellow crystals shown in Figure 4. Yield: 0.65 g (72%). ^{1}H NMR spectrographs are shown in results and discussion (Figures 8−10). The complex showed two forms in d_8-toluene solution. ^{1}H NMR (d_8-toluene, 400 MHz): Form A: δ 7.63 (1H, s, **H**C═N), 7.23−6.47 (m, ArH), 4.51 (2H, b, PhC**H$_2$**), 3.07 (2H, b, C═NC**H$_2$**), 2.22 (2H, b, C**H$_2$**NMe_2), 1.84 ppm (6H, s, N(C**H$_3$**)$_2$). Form B: δ 7.54 (1H, s, **H**C═N), 7.23−6.47 (m, ArH), 4.51 (2H, t, PhC**H$_2$**), 2.75 (2H, t, J = 6.4 Hz, C═NC**H$_2$**), 2.22 (6H, s, N(C**H$_3$**)$_2$), 2.08 ppm (2H, t, J = 6.4 Hz, C**H$_2$**NMe_2). The ratio of A and B was 4:1. Anal. Calcd (found) for $C_{36}H_{44}N_4O_4Zn_2$: C 59.43 (59.07), H 6.10 (6.18), N 7.70 (7.73)%.

Synthesis of $[L^2Zn(\mu\text{-OBn})]_2$ (2b). To a suspension of $[L^2ZnEt]_2$ (0.84 g, 1.25 mmol) in CH_2Cl_2 (15 mL) was added BnOH (0.31 mL, 3.0 mmol) at 0 °C. When the limpid yellow mixture was stirred for 3 h and a green yellow solution was obtained, volatile materials were removed in vacuo to yield the yellow powder. After adding 30 mL of hexane and washing the powder for 2 h, a yellow powder was collected by filtration. The yellow solid was dried in vacuo. The resulting yellow crystals shown in Figure 5 were collected in a NMR tube with $CDCl_3$. Yield: 0.57 g (55%). The complex showed three forms in $CDCl_3$ solution. ^{1}H NMR ($CDCl_3$, 600 MHz): (A) δ 9.11 (1H, s, **H**C═N), 7.89−7.02 (m, ArH), 4.92 (2H, b, PhC**H$_2$**), 3.71 (2H, t, J = 6.4 Hz, C═NC**H$_2$**), 2.54 (2H, J = 6.4 Hz, C**H$_2$**NMe_2), 2.08 ppm (6H, s, N(C**H$_3$**)$_2$). (B) δ 8.91 (1H, s, **H**C═N), 7.89−7.02 (m, ArH), 4.92 (2H, b, PhC**H$_2$**), 3.16 (2H, t, J = 5.6 Hz, C═NC**H$_2$**), 2.13 (2H, J = 5.6 Hz, C**H$_2$**NMe_2), 1.87 ppm (6H, s, N(C**H$_3$**)$_2$). (C) δ 8.84 (1H, s, **H**C═N), 7.89−7.02 (m, ArH), 4.92 (2H, b, PhC**H$_2$**), 3.29 (2H, b, C═NC**H$_2$**), 2.43 (2H, b, C**H$_2$**NMe_2), 2.39 ppm (6H, s, N(C**H$_3$**)$_2$). The ratio of A, B, and C is 7:1:3. Anal. Calcd (found) for $C_{44}H_{48}N_4O_4Zn_2\cdot 0.5CH_2Cl_2$: C 61.89 (62.04), H 5.71 (5.83), N 6.50 (6.35)%.

Synthesis of $[L^3Zn(\mu\text{-OBn})]_2$ (2c). To a suspension of $[L^3ZnEt]_2$ (0.80 g, 1.25 mmol) in the mixed solution (15 mL) of CH_2Cl_2 and THF was added BnOH (0.31 mL, 3.0 mmol) at 0 °C. When the limpid green yellow mixture was stirred for 3 h and a turbid solution was obtained, the light yellow powder was collected by filtration. After adding 30 mL of hexane and washing the powder for 2 h, a light yellow powder was collected by filtration. The light yellow solid was dried in vacuo. Yield: 0.45 g (45%). ^{1}H NMR ($CDCl_3$, 400 MHz): δ 8.11 (1H, s, **H**C═N), 7.34−7.27 (5H, m, $CH_2Ph\mathbf{H}_5$), 7.12 (1H, d, J = 8.0 Hz, Ar**H**), 7.00 (1H, s, Ar**H**), 6.75 (1H, d, J = 8.0 Hz, Ar**H**), 4.71 (2H, b, PhC**H$_2$**), 3.61 (2H, b, C═NC**H$_2$**), 2.53 (2H, b, C**H$_2$**NMe_2), 2.09 ppm (6H, s, N(C**H$_3$**)$_2$). ^{13}C NMR ($CDCl_3$, 400 MHz): δ 170.26 (**C**═N), 169.53 (**C**OH), 134.31, 133.33, 128.34, 127.04, 125.17, 118.74, 116.84 (Ar), 65.94 (O**C**H$_2$-Ph), 59.21 (CC═N**C**H$_2$), 56.74 (CC═NCH$_2$**C**H$_2$), 45.92 ppm (N(**C**H$_3$)$_2$). Anal. Calcd (found) for $C_{36}H_{42}Cl_2N_4O_4Zn_2$: C 54.29 (53.74), H 5.32 (4.93), N 7.03 (6.79)%.

Synthesis of $[L^4Zn(\mu\text{-OBn})]_2$(2d) and $[L^4{}_2Zn]$ (3). BnOH (0.31 mL, 3.0 mmol) was added to a suspension of $[L^4ZnEt]_2$ (0.91 g, 1.25 mmol) in a mixed solution (15 mL) of CH_2Cl_2 (7.5 mL) and THF (7.5 mL) at 0 °C. The resulting limpid yellow mixture was stirred for 3 h, during which the color of the solution changed to turbid solution; a light yellow powder was collected by filtration. After adding 30 mL of hexane and washing the powder for 2 h, a light yellow powder was collected by filtration. The light yellow solid was dried in vacuo. Yield: 0.72 g (65%). ^{1}H NMR ($CDCl_3$, 400 MHz): δ 8.11 (1H, s, **H**C═N), 7.34−7.26 (5H, m, $CH_2Ph\mathbf{H}_5$), 7.11 (1H, d, J = 9.2 Hz, Ar**H**), 6.99 (1H, s, Ar**H**), 6.74 (1H, d, J = 9.2 Hz, Ar**H**), 4.70 (2H, b, PhC**H$_2$**), 3.60 (2H, b, C═NC**H$_2$**), 2.54 (2H, b, C**H$_2$**NMe_2), 2.10 ppm (6H, s, N(C**H$_3$**)$_2$). ^{13}C NMR ($CDCl_3$, 400 MHz): δ 170.24 (**C**═N), 169.54 (**C**OH), 134.34, 133.36, 128.44, 127.42, 127.01, 125.17, 118.76, 116.87 (Ar), 65.99 (O**C**H$_2$Ph), 59.21 (CC═N**C**H$_2$), 56.80 (CC═NCH$_2$**C**H$_2$), 45.71 ppm (N(**C**H$_3$)$_2$). Anal. Calcd (found) for $C_{36}H_{42}Br_2N_4O_4Zn_2$: C 48.84 (49.08), H 4.78 (5.05), N 6.33 (6.55)%.

The crystals of $L^4{}_2Zn$ (**3**) were obtained from cooling a hot hexane solution of **2d**. The yield is too low to be measured.

Synthesis of $[L^5Zn(\mu\text{-OBn})]_2$ (2e). To a suspension of $[L^5ZnEt]_2$ (0.99 g, 1.25 mmol) in THF (15 mL) was added BnOH (0.31 mL, 3.0 mmol) at 0 °C. When the limpid yellow mixture was stirred for 3 h, volatile materials were removed in vacuo to yield a yellow powder. After adding 30 mL of hexane and washing the powder for 2 h, a yellow solution was collected by filtration. Volatile materials were removed in vacuo to yield a yellow powder. Yield: 0.41 g (35%). ^{1}H NMR ($CDCl_3$, 400 MHz): (A) δ 8.17 (1H, s, **H**C═N), 7.36 (1H, s, Ar**H**), 7.27−7.04 (5H, m, $CH_2Ph\mathbf{H}_5$), 6.86 (1H, s, Ar**H**), 4.84 (2H, b, PhC**H$_2$**), 3.57 (2H, t, J = 6.0 Hz, C═NC**H$_2$**), 2.09 (6H, s, N(C**H$_3$**)$_2$), 1.82 (2H, b, C**H$_2$**NMe_2), 1.36 (9H, $^pC(CH_3)_3$), 1.28 ppm (9H, $^oC(CH_3)_3$). (B) δ 7.87 (1H, s, **H**C═N), 7.43 (1H, s, Ar**H**), 7.27−7.04 (5H, m, $CH_2Ph\mathbf{H}_5$), 6.78 (1H, s, Ar**H**), 4.84 (2H, b, PhC**H$_2$**), 3.23 (2H, t, J = 5.6 Hz, C═NC**H$_2$**), 2.34 (2H, t, J = 5.6 Hz, C**H$_2$**NMe_2), 2.18 (6H, s, N(C**H$_3$**)$_2$), 1.57 (9H, $^pC(CH_3)_3$), 1.32 ppm (9H, $^oC(CH_3)_3$).

Synthesis of $[L^5Zn(\mu\text{-OCH}_2\text{CH}_2\text{NMe}_2)]_2$ (4). 2-(*N*,*N*-Dimethylamino)ethanol (0.30 mL, 3.0 mmol) was added to a suspension of $[L^5ZnEt]_2$ (0.99 g, 1.25 mmol) in THF (15 mL) at 0 °C. After the limpid yellow mixture was stirred for 3 h, volatile materials were removed in vacuo to yield yellow powder. The resulting powder was redissolved in hexane (20 mL) at 60 °C and filtered through Celite. The filtrate was then cooled to room temperature, giving

yellow crystals. The yellow crystals were collected by filtration. Yield: 0.45 g (40%). ^{1}H NMR (d_6-benzene, 400 MHz): δ 7.78 (1H, s, **H**C═N), 7.66 (1H, s, Ar**H**), 6.90 (1H, s, Ar**H**), 3.47 (2H, b, OC**H$_2$**), 3.11 (2H, b, C═NC**H$_2$**), 2.27−2.02 (8H, m, OCH$_2$C**H$_2$** + OCH$_2$CH$_2$N(C**H$_3$**)$_2$), 1.95 (2H, b, C═NCH$_2$C**H$_2$**), 1.86 (6H, s, N(C**H$_3$**)$_2$), 1.69 (9H, s, ^{p}C(C**H$_3$**)$_3$), 1.38 ppm (9H, s, ^{o}C(C**H$_3$**)$_3$). ^{13}C NMR (d_6-benzene, 400 MHz): δ 171.61 (**C**═N), 170.32 (**C**OH), 141.72, 133.83, 129.49, 129.17, 117.80 (Ar), 59.53 (CC═N**C**H$_2$), 58.75 (O**C**H$_2$), 57.26 (CC═NCH$_2$**C**H$_2$), 45.82, 45.09 (N(**C**H$_3$)$_2$), 35.88 (^{p}**C**(CH$_3$)$_3$), 33.94 (^{o}**C**(CH$_3$)$_3$), 31.53 (^{p}C(**C**H$_3$)$_3$), 30.04 ppm (^{o}C(C**H$_3$**)$_3$).

Melting Point Depression Measurement. [L^{1}Zn(μ-OBn)]$_2$ (2.00 g, 2.75 mmol) was dissolved in a hot naphthalene (15.00 g). The freezing point of the mixture was measured by slowly cooling the mixture, and the temperature was recorded once every 30 s using a Beckman thermometer, which was corrected prior to use. This procedure was repeated three times.

Typical Polymerization Procedure. A typical polymerization procedure was exemplified by the synthesis of PLA-75 using [L^{1}Zn(μ-OBn)]$_2$ as an initiator at 20 °C. The conversion yield (91%) of PLA was analyzed by ^{1}H NMR spectroscopic studies. A mixture of [L^{1}Zn(μ-OBn)]$_2$ (0.0377 g, 0.05 mmol) and L-lactide (1.08 g, 7.5 mmol) in toluene (20 mL) was stirred at 20 °C for 30 min. Volatile materials were removed in vacuo, and the residue was redissoved in THF (10 mL). The mixture was then quenched by the addition of an aqueous acetic acid solution (0.35 N, 10 mL), and the polymer was precipitated on pouring into *n*-hexane (40 mL) to give white crystalline solids. Yield: 0.82 g (76%).

X-ray Crystallographic Studies. Suitable crystals for X-ray structural determination were sealed in thin-walled glass capillaries under a nitrogen atmosphere and mounted on a Bruker AXS SMART 1000 diffractometer. Intensity data were collected in 1350 frames with increasing ω (width of 0.3° per frame). The absorption correction was based on the symmetry equivalent reflections using the SADABS program. The space group determination was based on a check of the Laue symmetry and systematic absences and was confirmed using the structure solution. The structure was solved by direct methods using a SHELXTL package. All non-H atoms were located from successive Fourier maps, and hydrogen atoms were refined using a riding model. Anisotropic thermal parameters were used for all non-H atoms, and fixed isotropic parameters were used for H atoms.

Acknowledgment. Financial support from the National Science Council of the Republic of China is gratefully appreciated.

Supporting Information Available: Crystallographic data (Suppl. Table 1) and tables giving full details of the crystal data. This material is available free of charge via the Internet at http://pubs.acs.org.

References and Notes

(1) (a) Endo, M.; Aida, T.; Inoue, S. *Macromo*lecules **1987**, *20*, 2982. (b) Duda, A.; Florjanczyk, Z.; Hofman, A.; Slomkowski, S.; Penczek, S. *Macromolecules* **1990**, *23*, 1640. (c) Kowalski, A.; Duda, A.; Penczek, S. *Macromol. Rapid Commun.* **1998**, *19*, 567. (d) Gan, Z.; Jim, T. F.; Jim, M.; Yuer, Z.; Wang, S.; Wu, C. *Macromolecules* **1999**, *32*, 1218. (e) Chamberlain, B. M.; Sun, Y.; Hagadorn, J. R.; Hemmesch, E. W.; Young, V. G., Jr.; Pink, M.; Hillmyer, M. A.; Tolman, W. B. *Macromolecules* **1999**, *32*, 2400. (f) Ovitt, T. M.; Coates, G. W. *J. Am. Chem. Soc.* **1999**, *121*, 4072. (g) Chen, X.; Gross, R. A. *Macromolecules* **1999**, *32*, 308. (h) Jeong, B.; Bae, Y. H.; Lee, D. S.; Kim, S. W. *Nature (London)* **1997**, *388*, 860. (i) Gref, R.; Minamitake, Y.; Peracchia, M. T.; Trubetskov, V.; Torchilin, V.; Langer, R. *Science* **1994**, *263*, 1600.

(2) (a) Ovitt, T. M.; Coates, G. W. *J. Am. Chem. Soc.* **2002**, *124*, 1316. (b) Huang, C.-H.; Wang, F.-C.; Ko, B.-T.; Yu, T.-L.; Lin, C.-C. *Macromolecules* **2001**, *34*, 356. (c) Liu, Y.-C.; Ko, B.-T.; Lin, C.-C. *Macromolecules* **2001**, *34*, 6196. (d) Chen, H.-L.; Ko, B.-T.; Huang, B.-H.; Lin, C.-C. *Organometallics* **2001**, *20*, 5076. (e) Hsueh, M.-L.; Huang, B.-H.; Lin, C.-C. *Macromolecules* **2002**, *35*, 5763. (f) Zhong, Z.; Dijkstra, P. J.; Feijen, J. *J. Am. Chem. Soc.* **2003**, *125*, 11291. (g) Radano, C. P.; Baker, G. L.; Smith, M. R. *J. Am. Chem. Soc.* **2000**, *122*, 1552. (h) Nomura, N.; Ishii, R.; Akakura, M.; Aoi, K. *J. Am. Chem. Soc.* **2002**, *124*, 5938. (i) Majerska, K.; Duda, A. *J. Am. Chem. Soc.* **2004**, *126*, 1026. (j) Chakraborty, D.; Chen, E. Y.-X. *Organometallics* **2002**, *21*, 1438. (k) Li, H.; Wang, C.; Bai, F.; Yue, J.; Woo, H.-G. *Organometallics* **2004**, *23*, 1411. (l) Doherty, S.; Errington, R. J.; Housley, N.; Clegg, W. *Organometallics* **2004**, *23*, 2382. (m) Lewińsk, J.; Horeglad, P.; Dranka, M.; Justyniak, I. *Inorg. Chem.* **2004**, *43*, 5789. (n) Lewiński, J.; Horeglad, P.; Wójcik, K.; Justyniak, I. *Organometallics* **2005**, *24*, 4588. (o) Chisholm, M. H.; Patmore, N. J.; Zhou, Z. *Chem. Commun.* **2005**, 127. (p) Lewiński, J.; Horeglad, P.; Tratkiewicz, E.; Grzenda, W.; Lipkowski, J.; Kolodziejczyk, E. *Macromol. Rapid Commun.* **2004**, *25*, 1939.

(3) (a) Kricheldorf, H. R. *Makromol. Chem.* **1993**, *194*, 1665. (b) Ko, B.-T.; Lin, C.-C. *J. Am. Chem. Soc.* **2001**, *123*, 7973. (c) Chisholm, M. H.; Lin, C.-C.; Galluccia, J. C.; Ko, B.-T. *Dalton Trans.* **2003**, 406.

(4) (a) Kricheldorf, H. R.; Berl, M.; Scharnagl, N. *Macromolecules* **1988**, *21*, 286. (b) Chisholm, M. H.; Eilerts, N. W.; Huffman, J. C.; Iyer, S. S.; Pacold, M.; Phomphrai, K. *J. Am. Chem. Soc.* **2000**, *122*, 11845. (c) Chisholm, M. H.; Gallucci, J.; Phomphrai, K. *Inorg. Chem.* **2002**, *41*, 2785. (d) Chisholm, M. H.; Phomphrai, K. *Inorg. Chim. Acta* **2003**, *350*, 121. (e) Chamberlain, B. M.; Cheng, M.; Moore, D. R.; Ovitt, T. M.; Lobkovsky, E. B.; Coates, G. W. *J. Am. Chem. Soc.* **2001**, *123*, 3229 (f) Marshall, E. L.; Gibson, V. C.; Rzepa, H. S. *J. Am. Chem. Soc.* **2005**, *127*, 6048.

(5) (a) O'Keefe, B. J.; Breyfogle, L. E.; Hillmyer, M. A.; Tolman, W. B. *J. Am. Chem. Soc.* **2002**, *124*, 4384. 6 (b) Duda, A.; Penczek, S. In *Polymers from Renewable Resources: Biopolyesters and Biocatalysis*; Scholz, C., Gross, R. A., Eds.; ACS Symposium Series Vol. 764. (c) Dobrzynski, P.; Kasperczyk, J.; Janeczek, M.; Bero, M. *Polymer* **2002**, *43*, 2595. (d) Wang, X.; Liao, K.; Quan, D.; Wu, Q. *Macromolecules* **2005**, *38*, 4611.

(6) (a) Kricheldorf, H. R.; Sumbbl, M. V.; Saunders, I. K. *Macromolecules* **1991**, *24*, 1944. (b) Aubrecht, K. B.; Hillmyer, M. A.; Tolman, W. B. *Macromolecules* **2002**, *35*, 644. (c) Amsden, B.; Wang, S.; Wyss, U. *Biomacromolecules* **2004**, *5*, 1399. (d) Nimitsiriwat, N.; Marshall, E. L.; Gibson, V. C.; Elsegood, M. R. J.; Dale, S. H. *J. Am. Chem. Soc.* **2004**, *126*, 13598.

(7) (a) Schwach, G.; Coudane, J.; Engel, R.; Vert, M. *Polym. Int.* **1998**, *46*, 177. (b) Bero, M.; Kasperczyk, J.; Jedliski, Z. *Macromol. Chem.* **1990**, *191*, 2287. (c) Bero, M.; Kasperczyk, J.; Adamus, G. *Macromol. Chem.* **1993**, *194*, 907.

(8) Chisholm, M. H.; Gallucci, J. C.; Zhen, H. *Inorg. Chem.* **2001**, *40*, 5051.

(9) See Supporting Information.

(10) See Supporting Information.

(11) (a) MacDonald, R. T.; McCarthy, S. P.; Gross, R. A. *Macromolecules* **1996**, *29*, 7356. (b) Stevels, W. M.; Ankone, M. J. K.; Dijkstra, P. J.; Feijen, J. *Macromolecules* **1996**, *29*, 6132. (c) Sarasua, J.-R.; Prud'homme, R. E.; Wisniewski, M.; Le Borgne, A.; Spassky, N. *Macromolecules* **1996**, *31*, 3895.

(12) Kasperczyk, J. E. *Macromolecules* **1995**, *28*, 3937.

(13) (a) Nakano, K.; Kosaka, N.; Hiyama, T.; Nozaki, K. *Dalton Trans.* **2003**, 4039. (b) Kricheldorf, H. R. *Polymer* **1992**, *33*, 2817. (c) O'Keefe, B. J.; Hillmyer, M. A.; Tolman, W. B. *Dalton Trans.* **2001**, 2215. (d) Cabaret, O. D.; Martin-Vaca, B.; Bourissou, D. *Chem. Rev.* **2004**, *104*, 6147.

(14) Villa, A. C.; Guastini, C.; Blech, P.; Floriani, C. *Dalton Trans.* **1990**, 3557.

(15) Cameron, P. A.; Gibson, V. C.; Redshaw, C.; Segal, J. A.; White, A. J. P.; Williams, D. J. *Dalton Trans.* **2002**, 415.

MA060471R